ACS OMEGA

http://pubs.acs.org/journal/acsodf

Article

Investigation of the Suppression of Methane Explosions by N_2/CO_2 Mixtures in Different Proportions

Xiaokun Chen, Tenglong Zhao,* Fangming Cheng, Kunlun Lu, Xueqiang Shi, and Wencong Yu

Cite This: *ACS Omega* 2023, 8, 10863−10874

Read Online

ACCESS | Metrics & More | Article Recommendations

ABSTRACT: To characterize the inerting effect of N_2/CO_2 mixtures containing various proportions on methane−air explosions, a series of experiments were conducted in a 20 L spherical vessel under the normal temperature (25 °C) and normal pressure (101 kPa). Six concentrations (10, 12, 14, 16, 18, and 20%) of N_2/CO_2 mixtures were selected to analyze the suppression of methane explosion by N_2/CO_2 mixtures. The results indicated that the maximum explosion pressure (p_{max}) of methane explosions was 0.501 MPa (17% N_2 + 3% CO_2), 0.487 MPa (14% N_2 + 6% CO_2), 0.477 MPa (10% N_2 + 10% CO_2), 0.461 MPa (6% N_2 + 14% CO_2), and 0.442 MPa (3% N_2 + 17% CO_2) in the presence of the same N_2/CO_2 concentration, and similar decreases in the rate of pressure rise, flame propagation velocity, and production of free radicals were observed. Therefore, with the increase of CO_2 concentration in the gas mixture, the inerting effect of N_2/CO_2 was enhanced. Meanwhile, the whole process of the methane combustion reaction was affected by N_2/CO_2 inerting, which was mainly attributed to heat absorption and dilution of the N_2/CO_2 mixture. N_2/CO_2 with a greater inerting effect leads to lower production of free radicals under the same explosion energy and a lower combustion reaction rate at the same flame propagation velocity. The findings of the current research provide references for the design of safe and reliable industrial processes and the mitigation of methane explosions.

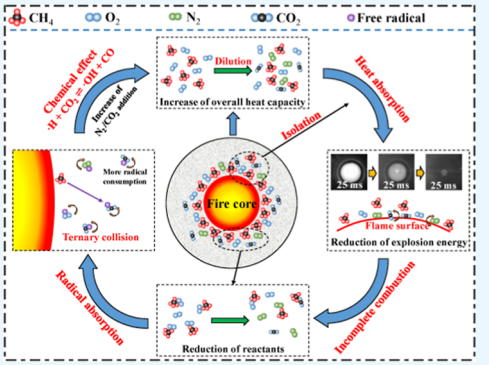

1. INTRODUCTION

Methane is an excellent alternative energy source for petroleum and an alternative fuel used in industry.[1,2] It plays an important role in the development of energy worldwide. As a high-quality fuel and chemical raw material, methane has a high combustion efficiency.[3] This provides energy for industrial manufacturing, and methane can also be used in organic curing reactions with hydrogen (H_2) to realize hydrogen storage and transport under easily accessible temperatures and pressures.[4−6] However, methane is highly combustible such that the methane−oxygen mixture is readily ignited.[7] During the transportation and use of methane, a certain concentration of methane will mix with air once a methane leakage occurs, leading to a methane explosion when encountering an open fire.[8−10] In the processing industry, the flammable gas and dust explosions have strong destructive power and present unpredictable risks in terms of equipment damage, environmental pollution, and casualties.[11−13] With the development of industrial technology, methane explosion accidents are inevitable and pose a huge threat to industrial safety, indicating the importance of preventing methane explosions.[14,15] Therefore, studies aiming to effectively prevent and control methane explosions are important.

Currently, one of the most efficient methods for reducing methane explosion hazards is using inert gases for suppression, most frequently N_2, CO_2, He, and Ar.[16−19] Among them, N_2 and CO_2 are commonly used to suppress combustible gas explosions due to their advantages of high efficiency, environmental friendliness, and convenience.[20−22] Numerous studies have been conducted to assess methane explosion suppression by N_2 and CO_2 and are summarized in publications. Di Benedetto[23] investigated the explosion behavior of a $CH_4/O_2/N_2/CO_2$ mixture with different CO_2 contents and oxygen air enrichment factors and observed that the main effect of CO_2 is on the specific heat of the mixture. Wang et al.[24] revealed that the explosion pressure and limiting oxygen concentration of methane explosion were reduced by N_2 and CO_2. According to Luo et al.,[25] the inerting effect of N_2 was better than that of CO_2 at high liquefied petroleum gas concentrations. Xie et al.[26] indicated that CO_2 participated in the chain reaction of methane combustion, leading to the incomplete combustion of methane. Furthermore, N_2 and CO_2 are both the main components of industrial exhaust gas produced by fossil fuel combustion.[27] Large amounts of N_2 and

Received: November 1, 2022
Accepted: March 6, 2023
Published: March 15, 2023

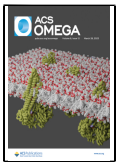

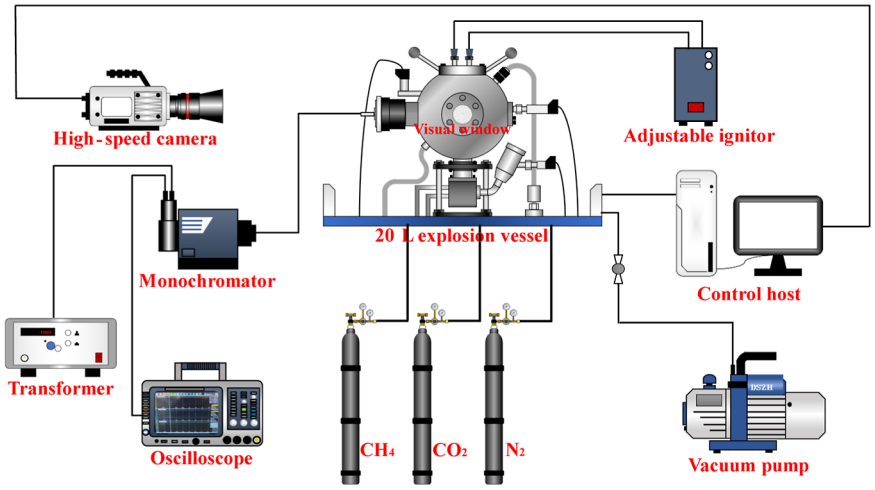

Figure 1. Experimental device.

CO_2 are present in these exhaust gases and their proportions vary, suggesting that they can also be used as excellent explosion suppressants.[28−30] In summary, previous investigations examining explosion mitigation mainly focused on an individual inert gas,[31,32] while fewer studies emphasized explosion suppression by the combination of N_2 and CO_2. The inerting effects of N_2/CO_2 mixtures with different proportions on methane explosions were yet to be fully understood. Moreover, previous studies mainly focused on the explosion pressure, rate of increase in pressure, flame temperature, and flame propagation velocity.[33−35] However, there were few studies on the radical production during explosions. The variation in different radical production during methane explosions under N_2/CO_2 suppression was still rare, and it was unclear whether some new phenomena exist in methane explosion suppression for the N_2/CO_2 mixture. Therefore, studies of explosion mitigation by N_2/CO_2 mixtures with different proportions are important and will be useful for the development of methane explosion prevention strategies. More detailed data are required to reveal the effect of N_2/CO_2 inerting on methane explosions.

In this study, N_2/CO_2 mixtures in various proportions were adopted to quantitatively analyze their effects on methane explosions. The inerting effect of N_2/CO_2 was tested in a 20 L spherical vessel, and parameters such as the explosion pressure, rate of increase in pressure, pressure characteristic time, and flame propagation velocity were obtained from the experiments. In addition, the production of different key radicals during methane explosion under N_2/CO_2 suppression was studied by recording the flame light radiation intensity at different wavelengths. Furthermore, based on kinetic and thermodynamic methods, a comparison of the explosion energy and production of free radicals was performed to reveal the effect of N_2/CO_2 on the methane combustion reaction. The study on the suppression of the CO_2/N_2 mixture on methane explosion is of significance for the recycling of exhaust gas. Meanwhile, the relevant results may provide basic data and references for the design of safe and reliable industrial processes and the prevention of methane explosions.

2. EXPERIMENTAL DETAILS

2.1. Experimental Facility. The detailed experimental setup is shown in Figure 1. It consisted of the following components: a 20 L spherical vessel, a high-speed camera, an oscilloscope, a transformer, a monochromator, a gas distribution device, an ignitor, a vacuum pump, and a control host. The 20 L spherical vessel was the reaction vessel used for methane explosions, with a pressure resistance of 4 MPa. The explosion pressure was measured by the pressure sensor located inside the vessel with a precision of 0.001 MPa. The sampling interval of the pressure sensor was 0.2 ms, and the total recording time was 3000 ms. The round window was composed of quartz, and the diameter of the window was 110 mm. An electric ignitor was employed in the center of the vessel for ignition, and the ignition energy was 18 J with a 300 ms arc duration. The gas distribution device was controlled by the control host, and the concentrations of CH_4, N_2, and CO_2 were calculated by Dalton's law of partial pressure.[36] The accuracy of the gas distribution device was 0.1%. The high-speed camera captured images of the explosion flame every 0.2 ms (5000 fps) from the window. The monochromator was used to record the flame light radiation intensity at different wavelengths. The optical signal obtained from the monochromator was converted into an electrical signal by the transformer and shown on the oscilloscope every 0.2 ms. The intensity of electrical signal was used to characterize the production of free radicals during methane explosion.

2.2. Experimental Materials and Methods. The flammable gas in this experiment was methane (CH_4, 99.99%), which was provided by Shaan'xi Qinlan Chemical Technology Co., Ltd., Shaanxi Province, China. The inert gases were carbon dioxide (CO_2 99.99%) and nitrogen (N_2, 99.99%), which were provided by Xi'an Yulong Gas CO., Ltd., Shaanxi Province, China. The experimental arrangement for all tests is listed in Table 1. In this study, methane with a stoichiometric concentration was used for explosion experiments, and thus, the concentration of methane was 9.5%. Six concentrations (10, 12, 14, 16, 18, and 20%) of N_2, CO_2, and N_2/CO_2 were selected to evaluate the methane explosion intensity in the CH_4-N_2/CO_2-air mixture. Five kinds of N_2/CO_2 were selected for further tests to fully understand the effects of N_2/CO_2 mixture proportions on inerting methane explosions. The explosion pressure and rate of increase in pressure were used to analyze the inerting effect of the inert gas mixture, and the flame propagation velocity was calculated to analyze the change in the methane combustion flame. Furthermore, the flame light radiation intensity was used to

https://doi.org/10.1021/acsomega.2c07053
ACS Omega 2023, 8, 10863−10874

Table 1. Summary of Experimental Scenarios

initial pressure (kPa)	equivalence ratio	vol. CH_4 (%)	vol. N_2 (%)	vol. CO_2 (%)
101	1.0	9.5	0	0
		9.5	10−20	0
		9.5	0	10−20
101	1.0	9.5	5	5
		9.5	6	6
		9.5	7	7
		9.5	8	8
		9.5	9	9
		9.5	10	10
		9.5	3	17
		9.5	6	14
		9.5	14	6
		9.5	17	3

characterize the radicals produced during methane explosion. All measurements were performed at ambient temperature (298 K) and pressure (101 kPa), and each experiment was repeated more than 3 times to ensure the accuracy of the experimental results.

Before the formal experiments, the maximum explosion pressure (p_{max}) of methane explosion under N_2/CO_2 suppression was measured. The p_{max} value was used to characterize the intensity of methane explosion. The decrease in the p_{max} value indicated that the intensity of methane explosion was reduced. When the p_{max} value was the standard atmospheric pressure, methane explosion did not occur. The experimental results are displayed in Figure 2. The p_{max} values

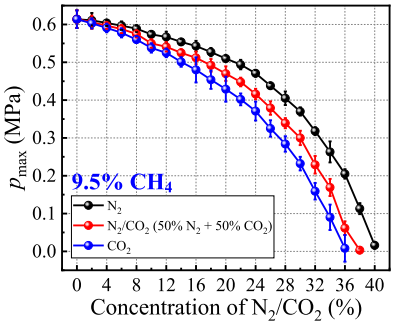

Figure 2. p_{max} of methane explosion with various concentrations of N_2/CO_2.

decreased rapidly as the addition of N_2/CO_2 increased. For the stoichiometric concentration of methane−air, the complete inerting concentrations of the N_2/CO_2 mixture were 40% (N_2), 37% (N_2/CO_2), and 36% (CO_2), respectively.

3. RESULTS AND DISCUSSION

3.1. Explosion Pressure. The explosion pressure and its rate of increase in the presence of various N_2/CO_2 concentrations were determined from the explosion pressure−time curves. Figure 3 displays the explosion pressure and history of the rate of increase in pressure with the stoichiometric methane−air mixture (9.5% CH_4). p_{max} is the maximum explosion pressure, and dp/dt_{max} is the maximum rate of increase in pressure. After a delay of 24 ms, the explosion pressure began to increase, and the rate gradually accelerated. p_{max} and dp/dt_{max} were achieved at the time of t_{max} and t_{vmax}. According to the curves, p_{max} and dp/dt_{max} of

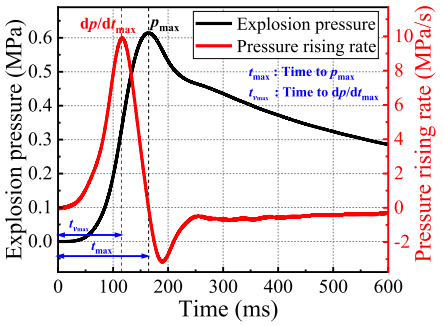

Figure 3. Curves of methane explosion pressure and pressure rising rate.

methane explosions were 0.614 MPa and 9.9 MPa/s, and t_{max} and t_{vmax} were 164.6 ms and 115.2 ms, respectively. The detailed analysis of the CH_4−N_2/CO_2−air mixture explosion is provided below.

Figure 4 shows the p_{max} of methane explosion with various N_2/CO_2 proportions and concentrations. Notably, p_{max} changed when N_2/CO_2 was added to the confined vessel. As the N_2/CO_2 concentration increased from 10 to 20%, p_{max} decreased from 0.599 MPa to 0.514 MPa (N_2), 0.561 MPa to 0.477 MPa (N_2/CO_2), and 0.534 MPa to 0.433 MPa (CO_2), respectively. The p_{max} value of the methane explosion decreased as the concentration of N_2/CO_2 increased, and the group exposed to 20% CO_2 had the lowest maximum explosion pressure. Meanwhile, the inerting effect is also affected by the proportion of N_2/CO_2. When adding 20% N_2/CO_2, the percent decrease ratios in p_{max} were 18.40% (17% N_2 + 3% CO_2), 20.68% (14% N_2 + 6% CO_2), 22.31% (10% N_2 + 10% CO_2), 24.92% (6% N_2 + 14% CO_2), and 28.01% (3% N_2 + 17% CO_2) compared to that with no inert gas mixture (as shown in Figure 4b). As a greater decrease in p_{max} occurred in the group treated with 17% CO_2, the explosion pressure decreased to a greater extent when more CO_2 was added to the gas mixture. Previous investigations suggested that the explosion pressure is related to the explosion energy.[37,38] The reduction in explosion pressure indicated a decrease in explosion energy. As the p_{max} value decreased to a greater extent, the N_2/CO_2 mixture with higher CO_2 concentrations had a greater inerting effect.

The variations in dp/dt_{max} with different N_2/CO_2 mixtures were studied and are shown in Figure 5. As the N_2/CO_2 concentration increased from 10% to 20%, dp/dt_{max} decreased from 9.141 MPa/s to 3.811 MPa/s (N_2), 5.873 MPa/s to 3.280 MPa/s (N_2/CO_2), and 3.450 MPa/s to 1.637 MPa/s (CO_2), respectively. The dp/dt_{max} value decreased more rapidly as more inert gas was added. The dp/dt_{max} value of the methane explosion was also affected by the proportions of the N_2/CO_2 mixture. When adding 20% N_2/CO_2, the percent decrease in dp/dt_{max} was 63.36% (17% N_2 + 3% CO_2), 64.95% (14% N_2 + 6% CO_2), 66.87% (10% N_2 + 10% CO_2), 74.31% (6% N_2 + 14% CO_2), and 80.67% (3% N_2 + 17% CO_2) compared to that without an inert gas mixture (as shown in Figure 5b). As the proportion of CO_2 in the gas mixture increased, dp/dt_{max} decreased to a greater extent. The decrease in the rate of increase in pressure indicates a reduction in the methane combustion reaction rate.[28,39] Thus, the addition of N_2/CO_2 suppresses methane combustion. In addition, the inerting effect of N_2/CO_2 on p_{max} was significantly greater than that on dp/dt_{max}. The main explanation for this result is that

https://doi.org/10.1021/acsomega.2c07053
ACS Omega 2023, 8, 10863−10874

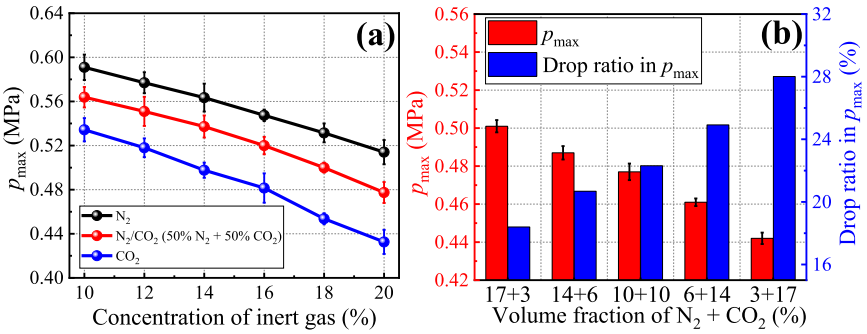

Figure 4. p_{max} of methane explosion with various concentrations of N_2/CO_2 (a) and various proportions of N_2/CO_2 (b).

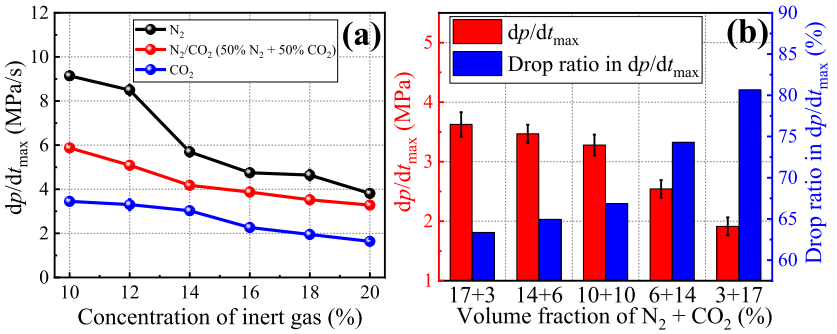

Figure 5. dp/dt_{max} of methane explosion with various concentrations of N_2/CO_2 (a) and various proportions of N_2/CO_2 (b).

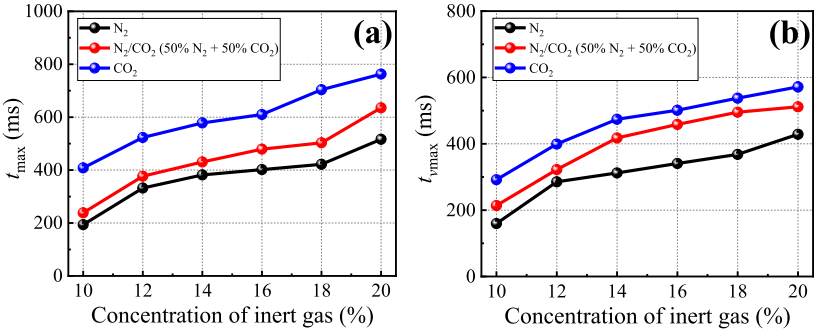

Figure 6. t_{max} (a) and t_{vmax} (b) of methane explosion with various concentrations of N_2/CO_2.

the reduction in the methane combustion reaction rate leads to a lower explosion intensity, but the explosion is not completely suppressed. Methane takes longer to be fully combusted, while the explosion energy decreases slightly.[40]

Figure 6 displays the two characteristic times (t_{max} and t_{vmax}) obtained with various N_2/CO_2 concentrations. As the N_2/CO_2 concentration increased from 10 to 20%, the t_{max} values increased from 193.8 to 516.4 ms (N_2), 238.4 to 635.2 ms (N_2/CO_2), and 408.4 to 762.8 ms (CO_2), and the t_{vmax} values increased from 159.6 to 428.8 ms (N_2), 214−511.6 ms (N_2/CO_2), and 291.8−571.6 ms (CO_2). As the N_2/CO_2 concentration increased, t_{max} and t_{vmax} were both prolonged. The delay of p_{max} indicated that the explosion energy increased slowly, while the delay of dp/dt_{max} indicated the decrease in the combustion reaction rate. A higher concentration of N_2/CO_2 helped further suppress the methane explosion. The variations in the two characteristic times with different N_2/CO_2 proportions were analyzed and are displayed in Figure 7. When adding 20% N_2/CO_2 mixtures, t_{max} was 543.8 ms (17% N_2 + 3% CO_2), 590.8 ms (14% N_2 + 6% CO_2), 635.2 ms (10% N_2 + 10% CO_2), 668.4 ms (6% N_2 + 14% CO_2), and 699.4 ms

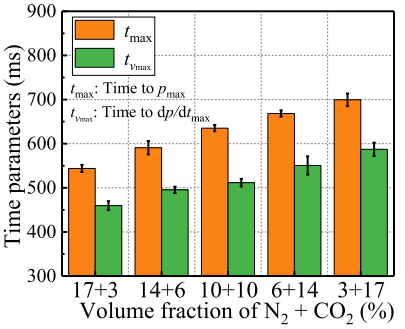

Figure 7. t_{max} and t_{vmax} of methane explosion with various proportions of N_2/CO_2.

(3% N_2 + 17% CO_2), and t_{vmax} was 459.6, 495.4, 511.6, 550.6, and 587.2 ms, respectively. The delay in the methane explosion was more obvious as the CO_2 proportion in the gas mixture increased. As more CO_2 was added to the gas mixture, the combustion reaction rate decreased, indicating slower explosive development. Therefore, the inhibitory effect is

https://doi.org/10.1021/acsomega.2c07053
ACS Omega 2023, 8, 10863−10874

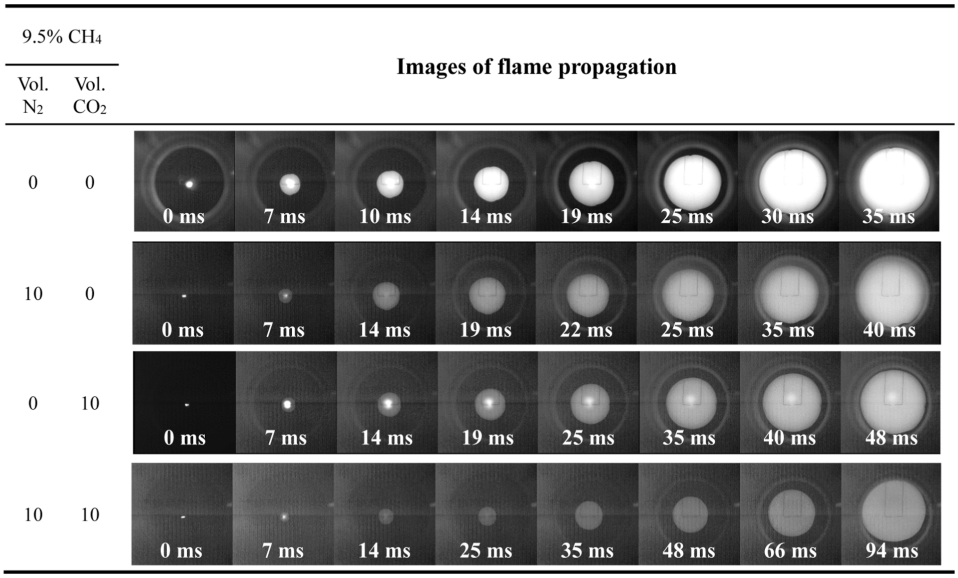

Figure 8. Flame propagation of the CH_4–N_2/CO_2–air mixture.

promoted with the increase in the CO_2 proportion in the N_2/CO_2 mixture.

3.2. Flame Propagation. Figure 8 displays the methane explosion flame propagation with different concentrations of N_2/CO_2. For methane explosions without N_2/CO_2, the flame became brighter and spread spherically at a variable velocity. The flame front arrived at the window boundary at 34 ms. For explosions with 10% N_2 or 10% CO_2, as the flame surface expanded, the concentration of O_2 around the flame surface decreased due to the dilution of N_2/CO_2. The insufficient O_2 caused incomplete combustion of methane, leading to a delay in flame propagation. The explosion flame arrived at the window boundary at 40 ms (10% N_2) and 48 ms (10% CO_2). For explosions in the presence of 10% N_2 + 10% CO_2, the shape of the flame surface was changed through the combined suppression by N_2 and CO_2. At 78 ms, the upward flame surface arrived at the window boundary, but the download flame was still spreading. At 112 ms, the downward flame surface arrived at the window boundary. Under N_2/CO_2 suppression, the explosion flame became weaker, and the time required for the flame front to reach the window boundary was significantly prolonged.

The velocity of flame propagation is one of the crucial parameters to determine the inerting effect of the N_2/CO_2 mixture.[41,42] A complete understanding of the flame dynamics is remarkably important. The flame propagation velocity was obtained from the flame images and calculated using eq 1[7,19,28]

$$u_H = \lim_{\Delta\tau\to 0}\frac{\Delta r}{\Delta\tau} = \frac{dr}{d\tau} = \frac{r_{\tau_2} - r_{\tau_1}}{\tau_2 - \tau_1} = \frac{1}{2}\frac{d_{\tau_2} - d_{\tau_1}}{\tau_2 - \tau_1} \quad (1)$$

where u_H is the flame propagation velocity, m/s; d is the diameter of the spherical flame, mm; r is the radius of the spherical flame, mm; and τ is the time of the flame propagation, ms. In this study, the velocity of upward flame propagation from the ignition arc to the window boundary was selected as the average flame propagation velocity (v_m) and used to analyze the effect of N_2/CO_2 on flame propagation. Figure 9 shows the method used to calculate the average flame propagation velocity. The vertical distance from the ignition electrode to the flame front was obtained from the flame

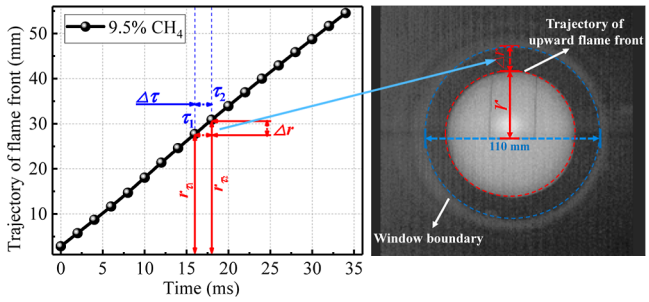

Figure 9. Calculation method of flame propagation velocity.

images, and the time at which the upward flame front reached the window boundary was recorded. As the upward flame front of the methane explosion without N_2/CO_2 arrived at the window boundary at 34.2 ms, the average flame propagation velocity of the unsuppressed methane explosion was 1.61 m/s.

Figure 10 depicts the average flame propagation velocity of the methane explosion (v_m) in the presence of varying concentrations of N_2/CO_2. For a 10% N_2/CO_2 gas mixture, the v_m value decreased from 1.61 to 1.38 m/s (10% N_2), 1.28 m/s (5% N_2 + 5% CO_2), and 1.15 m/s (10% CO_2), and the velocity was reduced by 14.29, 20.50, and 28.57%, respectively. When adding 20% N_2/CO_2, the percent decrease in v_m was 55.27, 65.22, and 68.94%, respectively. Flame propagation from the methane explosion was dramatically changed by N_2/CO_2 inerting. As the amount of N_2/CO_2 added increased, the flame propagation velocity was reduced to a larger degree. For the gas mixture with different proportions of N_2/CO_2, the inerting effect of N_2/CO_2 varied. As shown in Figure 10b, in the presence of the same concentration of N_2/CO_2, the average flame propagation velocities were 0.67 m/s (17% N_2 + 3% CO_2), 0.625 m/s (14% N_2 + 6% CO_2), 0.56 m/s (10% N_2 + 10% CO_2), 0.51 m/s (6% N_2 + 14% CO_2), and 0.505 m/s (17% N_2 + 3% CO_2). As more CO_2 was added to the N_2/CO_2 mixture, the flame propagation velocity decreased significantly. Thus, the inerting effect of CO_2 is more prominent than that of N_2 in the inert gas mixture.

3.3. Radical Production. Previous investigations have shown that the production of different free radicals can be

https://doi.org/10.1021/acsomega.2c07053
ACS Omega 2023, 8, 10863−10874

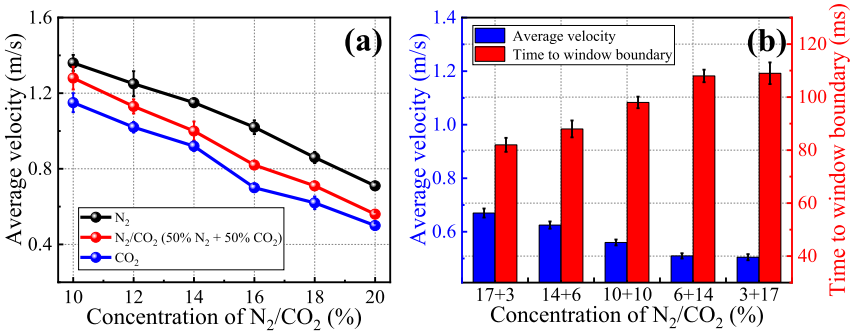

Figure 10. Average flame propagation velocity of methane explosion with various concentrations of N_2/CO_2 (a) and various proportions of N_2/CO_2 (b).

recorded by monitoring the variations in flame light radiation intensity at different wavelengths (the intensity of free radical emission spectra) during methane combustion.[43] In this experiment, a monochromator was used to monitor the emission spectra of different free radicals and fully understand the effect of N_2/CO_2 on the methane combustion reaction. Nine free radicals were selected and set as $\lambda(^{\bullet}H)$ = 656.25 nm, $\lambda(^{\bullet}CH_2O)$ = 412.1 nm, $\lambda(^{\bullet}OH)$ = 306.36 nm, $\lambda(^{\bullet}CH)$ = 314.5 nm, $\lambda(^{\bullet}CN)$ = 359.0 nm, $\lambda(^{\bullet}CHO)$ = 318.6 nm, $\lambda(^{\bullet}O)$ = 470.5 nm, $\lambda(^{\bullet}NO)$ = 237.02 nm, and $\lambda(^{\bullet}CO)$ = 199.09 nm.[44−48] The maximum intensity of flame light radiation (U_{max}) was used to characterize radical production. Figure 11

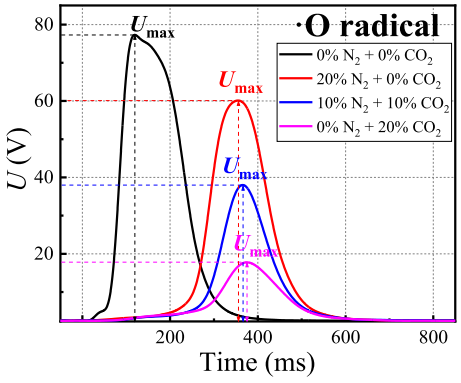

Figure 11. Flame light radiation intensity curves of methane explosion under N_2/CO_2 suppression ($^{\bullet}O$ radical).

displays the flame light radiation intensity of the $^{\bullet}O$ radical and its variation in explosions containing various proportions of N_2/CO_2. The U_{max} value of the $^{\bullet}O$ radical decreased, while the time to U_{max} was significantly prolonged as N_2/CO_2 was added. The reduction in $^{\bullet}O$ radical production indicated that O_2 consumption decreased during the explosion, and thus, the methane combustion reaction was suppressed. When adding N_2/CO_2 in the confined vessel, the concentration of O_2 decreased, indicating a reduction in the level of reactant available for the methane combustion reaction.[49] In addition, the minimum U_{max} value was observed when 20% CO_2 was added, which was mainly attributed to the physical and chemical properties of N_2 and CO_2. According to chain reaction theory, as high-energy free radicals collide with N_2 or CO_2 molecules, the energy from radicals is transferred to inert gas molecules. When adding more N_2/CO_2, the probability of ternary collision increases, leading to reduced production of free radicals.[50] This energy absorption capacity is related to the heat capacity of the inert gas. With the addition of N_2/CO_2, the overall specific heat capacity in the confined vessel increased. More explosion energy was consumed by N_2/CO_2, and thus, the methane combustion reaction rate was reduced at lower flame temperatures.[51] Meanwhile, because the volumetric specific heat capacity of CO_2 is greater than that of N_2, the group with a higher CO_2 concentration had a better heat absorption capacity.[52] Thus, the group treated with 20% CO_2 produces a lower amount of $^{\bullet}O$ radicals.

The variations in the levels of the nine free radicals with different concentrations of N_2/CO_2 were obtained, and the results are displayed in Figure 12. When adding a 20% N_2/CO_2 mixture (10% N_2 + 10% CO_2), the percent decrease in U_{max} was 36.98, 40.37, 39.76, 38.83, 32.04, 38.19, 64.59, 52.51, and 34.03%, respectively. As the concentration of N_2/CO_2 increased, the U_{max} value decreased to a larger degree. The detailed data associated with the percent decrease in U_{max} are shown in Table 2. All U_{max} values decreased with the addition of N_2/CO_2. As free radicals, such as $^{\bullet}O$, $^{\bullet}H$, and $^{\bullet}OH$ radicals, affect the consumption of methane molecules, the reduced levels of these radicals indicated that a considerable part of methane in the confined vessel was not consumed during combustion.[53] Similarly, the reduced levels of C-containing radicals, such as $^{\bullet}CO$, $^{\bullet}CH$, $^{\bullet}CHO$, and $^{\bullet}CH_2O$, indicated that some methane did not participate in the combustion reaction. Furthermore, the suppression of $^{\bullet}CN$ and $^{\bullet}NO$ radical production proved that the addition of N_2 did not promote the formation of N-containing radicals during combustion. The whole process of the methane combustion reaction was affected by the inert gas mixture. As the N_2/CO_2 concentration increased, the inerting effect of N_2/CO_2 was enhanced, and the production of the key free radicals was reduced.

The variation in radical production with different N_2/CO_2 proportions is displayed in Figure 13. The radicals produced during the methane explosion were affected by the proportions of the N_2/CO_2 mixture at the same inert gas concentration. The detailed data associated with U_{max} values obtained with various N_2/CO_2 proportions are shown in Table 3. For example, the U_{max} value of the $^{\bullet}O$ radical was 54.33 V (17% N_2 + 3% CO_2), 49.84 V (14% N_2 + 6% CO_2), 38.01 V (10% N_2 + 10% CO_2), 22.95 V (6% N_2 + 14% CO_2), and 20.16 V (17% N_2 + 3% CO_2). The reduction in $^{\bullet}O$ radical production might be attributed to the decrease in the O_2 concentration; meanwhile, the reduction in the collision probability of methane molecules and oxygen molecules also inhibited $^{\bullet}O$ radical production.[54] As CO_2 inerting was greater than that of N_2, the production of $^{\bullet}O$ radicals decreased to a greater extent as the proportion of CO_2 in the N_2/CO_2 mixture increased.

https://doi.org/10.1021/acsomega.2c07053
ACS Omega 2023, 8, 10863−10874

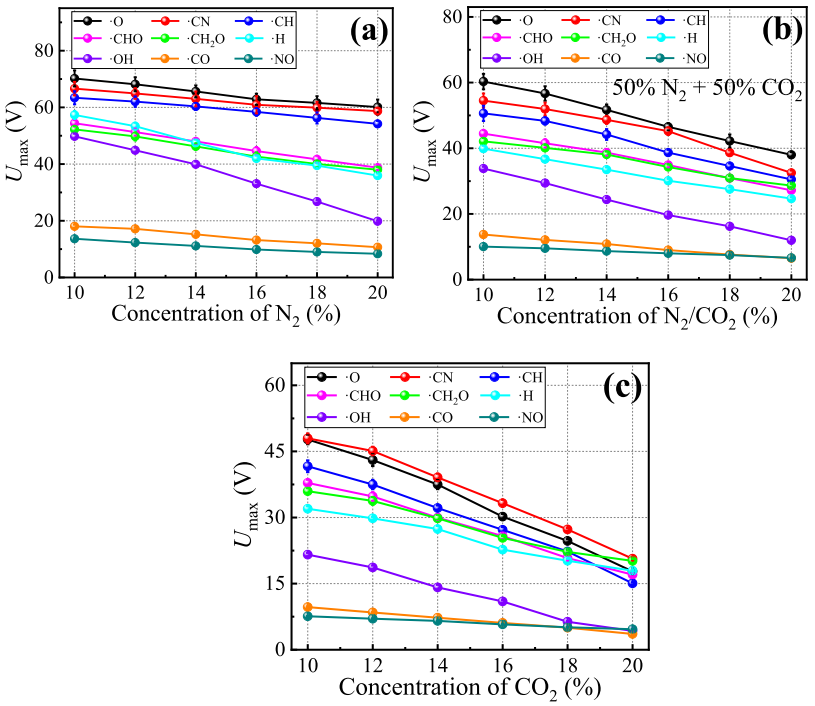

Figure 12. U_{max} of methane explosion with various concentrations of N_2 (a), N_2/CO_2 (b), and CO_2 (c).

Table 2. Drop Ratios in U_{max} at Different Wavelengths of Methane Explosion with the Same N_2/CO_2 Concentration

		drop ratio in maximum flame light radiation intensity (%)								
vol. N_2	vol. CO_2	•O	•CN	•CH	•CHO	•CH_2O	•H	•OH	•CO	•NO
20	0	14.36	11.88	14.53	28.77	27.24	37.29	60.16	40.94	38.68
10	10	36.98	40.37	39.76	38.83	32.04	38.19	64.59	52.51	34.03
0	20	62.76	56.92	63.82	54.98	43.97	43.9	80.12	62.87	38.6

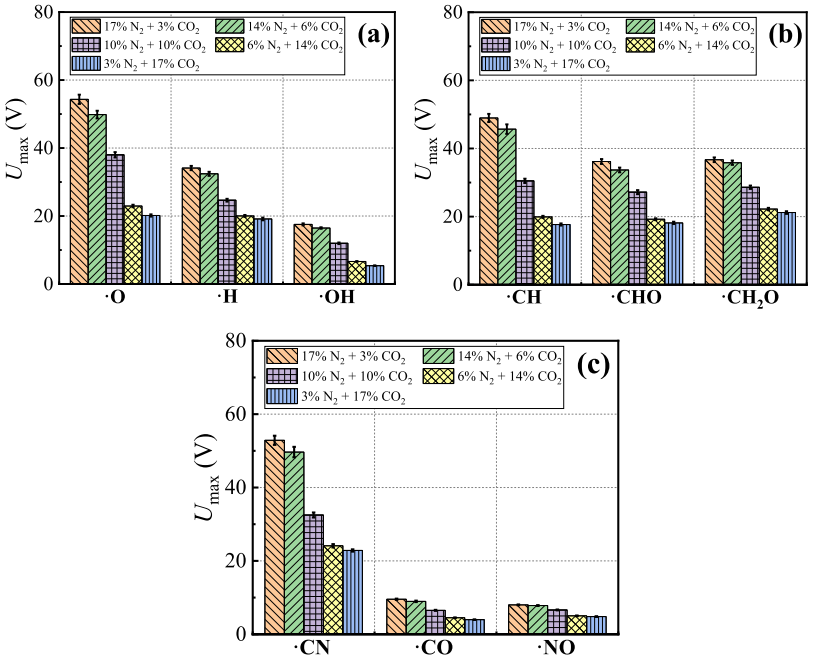

Figure 13. U_{max} of •O, •H, •OH radical (a), •CH, •CHO, •CH_2O radical (b), and •CH, •CHO, •CH_2O radical (c).

Notably, the U_{max} value of the •H radical was 54.33 V (17% N_2 + 3% CO_2), 49.84 V (14% N_2 + 6% CO_2), 38.01 V (10% N_2 + 10% CO_2), 22.95 V (6% N_2 + 14% CO_2), and 20.16 V (17% N_2 + 3% CO_2). Specifically, CO_2 participates in the methane combustion reaction through the elementary reaction •H + CO_2 ⇌ •OH + CO.[26] More •H radicals are consumed by CO_2,

https://doi.org/10.1021/acsomega.2c07053
ACS Omega 2023, 8, 10863−10874

Table 3. U_{max} at Different Wavelengths of Methane Explosion with the Same N_2/CO_2 Concentration

		maximum flame light radiation intensity (V)								
vol. N_2 (%)	vol. CO_2 (%)	•O	•CN	•CH	•CHO	•CH_2O	•H	•OH	•CO	•NO
17	3	54.33	52.87	48.95	36.17	36.69	34.11	17.54	9.54	8.01
14	6	49.84	49.67	45.68	33.69	35.82	32.41	16.47	8.97	7.83
10	10	38.01	32.51	30.5	27.19	28.62	24.65	11.98	6.52	6.63
6	14	22.95	24.11	19.92	19.23	22.21	20.02	6.63	4.5	5.02
3	17	20.16	22.84	17.68	18.15	21.19	19.15	5.39	3.99	4.81

leading to the reduction of •H radicals involved in methane combustion. Moreover, the addition of the N_2/CO_2 mixture leads to the incomplete combustion of methane, which further suppresses the methane explosion.[28] By comparing the results for the production of nine radicals, it can be found that as the CO_2 proportion in the N_2/CO_2 mixture increased, the amounts of all radicals produced decreased. Therefore, the production of key free radicals might be effectively inhibited by N_2/CO_2 inactivation. As the proportion of CO_2 in the gas mixture increased, the inhibition of radical production gradually increased. In addition, the thermal dissociation of CO_2 occurred at high temperature, and its main products were CO and O_2. With the addition of the N_2/CO_2 mixture, the heat generated by methane combustion decreased, which inhibited the thermal dissociation of CO_2. The decreased production of CO and O_2 further suppressed methane explosion.

3.4. Correlation Analysis. The relationships between explosion energy and radical production, as well as flame propagation and combustion reaction rate, are discussed in this section. According to previous investigations, the explosion pressure is related to the explosion energy, and the rate of increase in the pressure is related to the combustion reaction rate. The production of free radicals was affected by the explosion energy, and flame propagation was affected by the combustion reaction rate. In this study, p_{max} was used to characterize the explosion energy, and U_{max} was calculated to characterize the production of free radicals. The relationship between p_{max} and U_{max} for the •O radical is displayed in Figure 14. Notably, p_{max} basically exhibited a linear relationship with

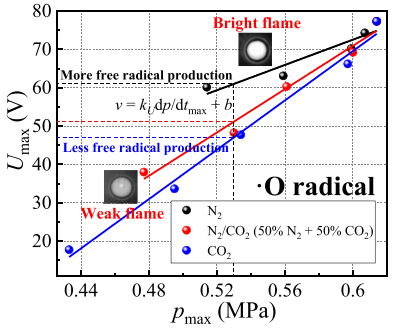

Figure 14. Relationship of p_{max} and U_{max} of methane explosion under N_2/CO_2 suppression.

U_{max}. First, at the same p_{max} value, the U_{max} value of the group exposed to 20% CO_2 was significantly lower than that of the other two groups, indicating a lower amount of radical production at the same explosion energy. Therefore, the N_2/CO_2 mixture with a greater inerting effect has a greater capacity to inhibit radical production at the same explosion intensity. Second, as p_{max} increased, the U_{max} value obtained with different proportions of N_2/CO_2 inerting increased to varying degrees. Assuming that p_{max} and U_{max} were linear, the relationship between p_{max} and U_{max} for •O radicals was calculated using eq 2

$$U_{max} = k_U p_{max} + b \quad (2)$$

where k_U is the slope of the fitting line, which indicates the effect of the explosion energy on radical production. The larger the value of k_U, the greater the effect of the explosion energy on radical production. The slope values of the fitting lines for different radicals are shown in Figure 15. For •O radicals, the k_U values were 26.27 (20% N_2), 98.47 (10% N_2 + 10% CO_2), and 123.38 (20% CO_2). As the proportion of CO_2 in the N_2/CO_2 mixture increased, the effect of the explosion energy on radical production increased. Similar results were obtained from the analysis of nine radicals, indicating the effect of the N_2/CO_2 mixture on inhibiting radical production. Therefore, the N_2/CO_2 mixture exerts a significant effect on radical production, and the mixture with greater inerting leads to lower production of free radicals at the same explosion energy.

In addition, dp/dt_{max} was selected as the parameter to characterize the combustion reaction rate. The relationship between the combustion reaction rate and flame propagation velocity was discussed, and the results are displayed in Figure 16. In this figure, dp/dt_{max} basically exhibited a linear relationship to the flame propagation velocity. At the same flame propagation velocity, the group with a greater inerting effect had a lower dp/dt_{max} value, indicating a reduction in the combustion reaction rate. Assuming that dp/dt_{max} and flame propagation velocity were linear, the relationship between them was calculated using eq 3

$$v_m = k_v dp/dt_{max} + b \quad (3)$$

where k_v is the slope of the fitting line, which was used to characterize the relationship of the combustion reaction rate and flame propagation velocity. As shown in Figure 16b, the k_v values were 0.10 (20% N_2), 0.25 (10% N_2 + 10% CO_2), and 0.33 (20% CO_2). As the concentration of the N_2/CO_2 mixture increased, the flame propagation velocity of the group containing more CO_2 decreased more rapidly. Therefore, at the same flame propagation velocity, the N_2/CO_2 mixture with a greater inerting effect would lead to a lower combustion reaction rate.

By comparing the experimental results with the analytical results, it can be found that the N_2/CO_2 mixture displayed an excellent inerting effect of methane explosions, which was mainly reflected in the reductions in explosion pressure and methane combustion reaction rate. The production of different free radicals was reduced under N_2/CO_2 inerting, so the methane combustion reaction had more difficulty in proceeding, and the intensity of methane explosion was further weakened. Furthermore, methane explosion flame propagation was suppressed under N_2/CO_2 inerting. As the flame

https://doi.org/10.1021/acsomega.2c07053
ACS Omega 2023, 8, 10863−10874

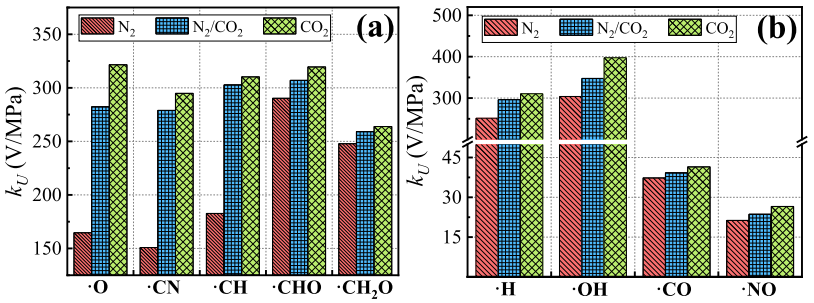

Figure 15. k_U of •O, •CN, •CH, •CHO, •CH_2O radical (a) and •H, •OH, •CO, •NO radical (b).

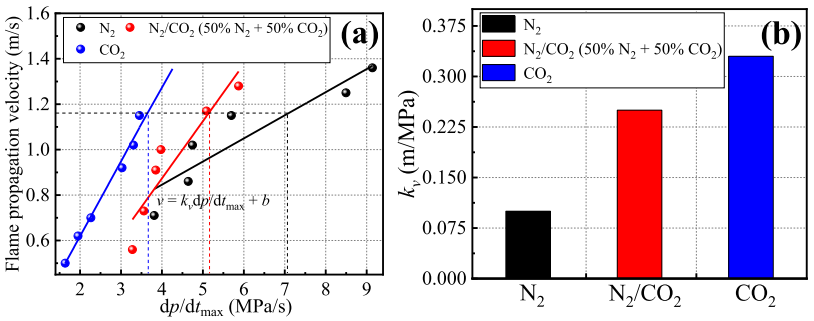

Figure 16. Fitting lines (a) and k_v (b) of flame propagation velocity and combustion reaction rate.

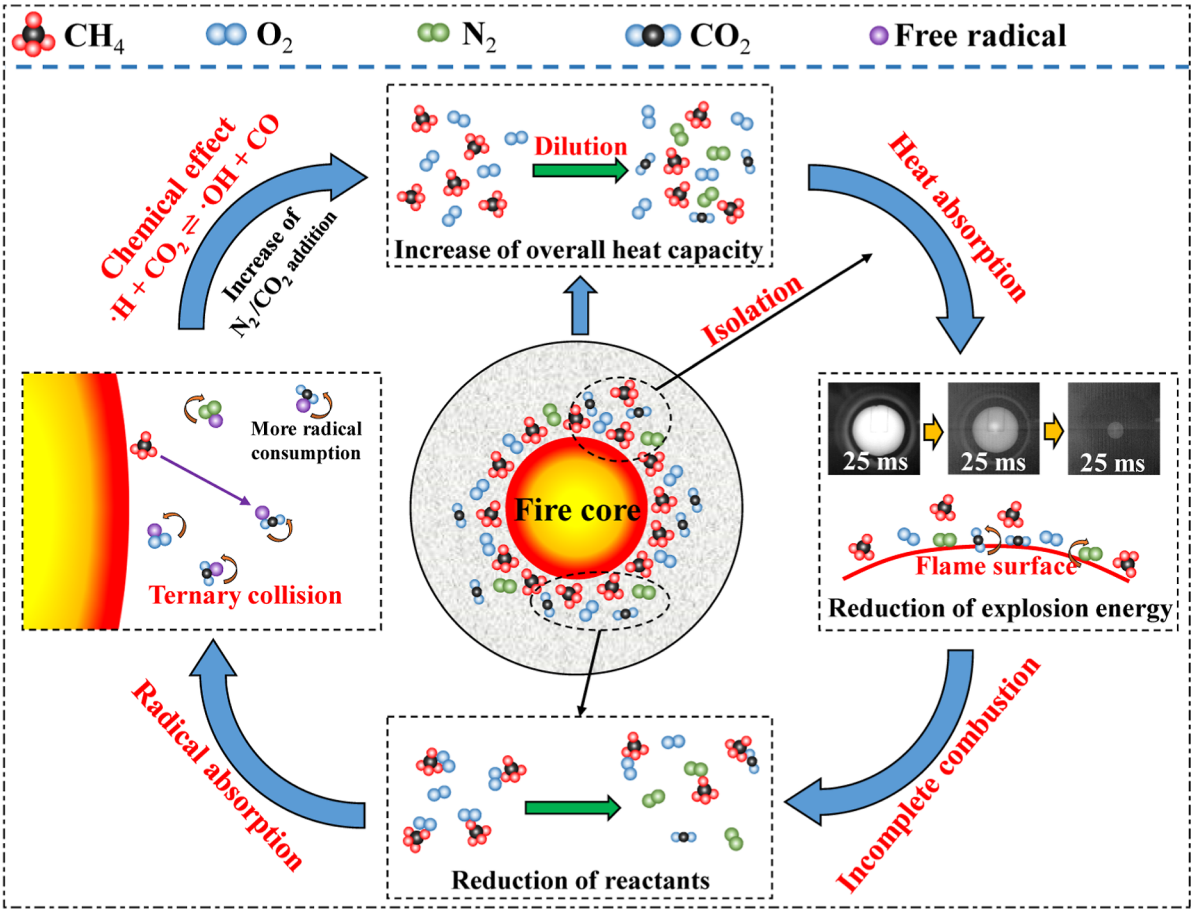

Figure 17. Synergistic inhibition process of the N_2/CO_2 mixture on methane explosion.

propagated, more heat generated by methane combustion was absorbed by N_2 and CO_2 molecules, and the energy absorbed by methane combustion was further reduced. Meanwhile, the N_2/CO_2 mixture with a greater inerting effect made the radical production and combustion reaction rate decrease to a larger degree. Therefore, the N_2/CO_2 mixture influenced all

https://doi.org/10.1021/acsomega.2c07053
ACS Omega 2023, 8, 10863−10874

flammability parameters, such as the explosion pressure, rate of pressure rise, and laminar burning velocity, and the whole process of the methane combustion reaction was affected by N_2/CO_2 inerting. Based on the aforementioned discussion, the synergistic inhibitory mechanism of the N_2/CO_2 mixture is displayed in Figure 17. The overall specific heat capacity of the gas mixture increased with the addition of N_2/CO_2, which led to the consumption of a large amount of heat produced by the explosion, thus reducing the explosion energy. Meanwhile, the production of most radicals was reduced under N_2/CO_2 inerting, which was mainly attributed to the reduction in the levels of reactants involved in the combustion reaction. First, the O_2 concentration in the vessel decreased as N_2/CO_2 was added, leading to the incomplete combustion of methane. Second, as the explosion energy decreased, more methane molecules were unable to participate in the combustion reaction. Based on these results, the methane explosion intensity was further weakened. Notably, the specific heat capacity of CO_2 is higher than that of N_2, indicating a greater heat absorption of CO_2 following the addition of the same amount of the gases. Furthermore, CO_2 participated in the methane combustion reaction through the elementary reaction $^{\bullet}H + CO_2 \rightleftharpoons {}^{\bullet}OH + CO$, resulting in the reduction of $^{\bullet}H$ radicals involved in methane combustion. Thus, the inerting effect of N_2/CO_2 was improved as the proportion of CO_2 increased.

4. CONCLUSIONS

In this study, the inerting effect of CO_2/N_2 on methane explosion was comprehensively analyzed by comparing the explosion pressure, flame propagation velocity, and production of free radicals. The main conclusions are summarized below.

The parameters of methane explosion with various proportions of the N_2/CO_2 mixture, such as explosion pressure and rate of increase in pressure, were obtained, and the inerting effect of the inert gas mixture was characterized by these parameters. For 20% N_2/CO_2, the p_{max} values of the gas mixture explosion are 0.501 MPa (17% N_2 + 3% CO_2), 0.487 MPa (14% N_2 + 6% CO_2), 0.477 MPa (10% N_2 + 10% CO_2), 0.461 MPa (6% N_2 + 14% CO_2), and 0.442 MPa (3% N_2 + 17% CO_2), and the dp/dt_{max} values are 3.627, 3.47, 3.28, 2.543, and 1.914 MPa/s, respectively. The inerting effect of N_2/CO_2 improves as the proportion of CO_2 in the inert gas mixture increases.

The variations in radical production during the methane explosion under N_2/CO_2 inerting are clarified. N_2/CO_2 inerting plays an important role in suppressing methane explosions, which exerts a significant effect on the methane combustion reaction. As the N_2/CO_2 concentration increases, the flame light radiation intensity at different wavelengths decreases, indicating a reduction in key free radical production ($^{\bullet}H$, $^{\bullet}CH_2O$, and $^{\bullet}OH$). The addition of N_2/CO_2 leads to a decrease in the O_2 concentration, and the heat absorption of N_2/CO_2 prevents more methane in the confined vessel from participating in the combustion reaction.

The relationship between the explosion energy and radical production is discussed. At the same explosion energy, N_2/CO_2 with a greater inerting effect will lead to a lower production of free radicals. Meanwhile, the relationship between the flame propagation velocity and combustion reaction rate is discussed. At the same flame propagation velocity, N_2/CO_2 with a greater inerting effect will lead to a lower combustion reaction rate. The explosion energy and methane combustion reaction rate are affected by N_2/CO_2 inerting. As the proportion of CO_2 in the N_2/CO_2 mixture increases, the explosion energy and combustion reaction rate are both reduced to a larger degree.

AUTHOR INFORMATION

Corresponding Author

Tenglong Zhao − *School of Safety Science and Engineering, Xi'an University of Science and Technology, Xi'an, Shaanxi 710054, PR China;* orcid.org/0000-0001-5700-6321; Email: zhaotenglong@stu.xust.edu.cn

Authors

Xiaokun Chen − *School of Safety Science and Engineering and Shaanxi Key Laboratory of Prevention and Control of Coal Fire, Xi'an University of Science and Technology, Xi'an, Shaanxi 710054, PR China*

Fangming Cheng − *School of Safety Science and Engineering and Shaanxi Key Laboratory of Prevention and Control of Coal Fire, Xi'an University of Science and Technology, Xi'an, Shaanxi 710054, PR China*

Kunlun Lu − *School of Safety Science and Engineering, Xi'an University of Science and Technology, Xi'an, Shaanxi 710054, PR China; School of Chemistry and Environmental Engineering, Sichuan University of Science and Engineering, Zigong, Sichuan 643000, PR China;* orcid.org/0000-0003-3567-5051

Xueqiang Shi − *School of Safety Science and Engineering, Xi'an University of Science and Technology, Xi'an, Shaanxi 710054, PR China;* orcid.org/0000-0001-8649-3878

Wencong Yu − *School of Safety Science and Engineering, Xi'an University of Science and Technology, Xi'an, Shaanxi 710054, PR China*

Complete contact information is available at: https://pubs.acs.org/10.1021/acsomega.2c07053

Notes

The authors declare no competing financial interest.

ACKNOWLEDGMENTS

This study was supported by the National Natural Science Foundation of China (no. 52174208), the National Natural Science Foundation of China (no. 52004208), and the Natural Science Basic Research Program of Shaanxi (no. 2021JQ-565).

REFERENCES

(1) Zhao, K.; Wang, Z. R.; Ma, C.; Cao, X. Y.; Guo, P. K.; Guo, W. J.; Lu, Y. W. Experimental study on the domino effect in explosions caused by vertically distributed methane/air vapor clouds. *Fuel* **2021**, *290*, 120014.

(2) Elbaz, A. M.; Roberts, W. L. Investigation of the effects of quarl and initial conditions on swirling non-premixed methane flames: flow field, temperature, and species distributions. *Fuel* **2016**, *169*, 120−134.

(3) Mitu, M.; Razus, D.; Schroeder, V. Laminar Burning Velocities of Hydrogen-Blended Methane−Air and Natural Gas-Air Mixtures, Calculated from the Early Stage of p(t) Records in a Spherical Vessel. *Energies* **2021**, *14*, 7556.

(4) Cao, W. G.; Liu, Y. F.; Chen, R. K.; Li, W. J.; Zhang, Y.; Xu, S.; Cao, X.; Huang, Q.; Tan, Y. X. Pressure release characteristics of premixed hydrogen-air mixtures in an explosion venting device with duct. *Int. J. Hydrogen Energy* **2021**, *46*, 8810−8819.

(5) Wang, Z. H.; Shui, K.; You, F.; Dederichs, A. S.; Markert, F.; Jiang, J. C.; Zhang, Y.; Li, D.; Fu, Z. L.; Xu, J. X.; He, L.; Huangfu, W.

H. Prediction of the failure probability of the overhead power line exposed to large-scale jet fires induced by high-pressure gas leakage. *Int. J. Hydrogen Energy* **2021**, *46*, 2413−2431.
(6) Jiang, Y. M.; Pan, X. H.; Zhang, T.; Wang, Z. L.; Wang, Q. Y.; Ta, L.; Li, Y. Y.; Hua, M.; Zhang, B.; Jiang, J. C. Experimental study on pressure and flow characteristics of self-ignition hydrogen flowing into the unconfined space. *Process Saf. Environ.* **2022**, *159*, 120−132.
(7) Akram, M.; Kumar, S.; Saxena, P. Experimental and computational determination of laminar burning velocity of liquefied petroleum gas-air mixtures at elevated temperatures. *J. Eng. Gas Turbines Power* **2013**, *135*, 091501.
(8) Wang, K.; Pan, H. Y.; Zhang, T. J.; Wang, H. T. Experimental study on the radial vibration characteristics of a coal briquette in each stage of its life cycle under the action of CO_2 gas explosion. *Fuel* **2022**, *320*, 123922.
(9) Prodan, M.; Mitu, M.; Razus, D.; Oancea, D. Spark ignition and propagation properties of methane-air mixtures from early stages of pressure history. *Rev. Roum. Chim.* **2016**, *61*, 299−305.
(10) Cao, W. G.; Zhou, Z. H.; Li, W. J.; Zhao, Y. M.; Yang, Z. X.; Zhang, Y.; Ouyang, S. M.; Shu, C. M.; Tan, Y. X. Under-expansion jet flame propagation characteristics of premixed H_2/air in explosion venting. *Int. J. Hydrogen Energy* **2021**, *46*, 38913−38922.
(11) Shi, X. Q.; Chen, X. K.; Zhang, Y. T.; Zhang, Y. B.; Guo, R. Z.; Zhao, T. L.; Liu, R. Numerical simulation of coal dust self-ignition and combustion under inclination conditions. *Energy* **2022**, *239*, 122227.
(12) Wen, H.; Mi, W. S.; Fan, S. X.; Liu, M. Y.; Cheng, X. J.; Wang, H. Determining the reasonable volume required to inject liquid CO_2 into a single hole and displace CH_4 within the coal seam in bedding boreholes: case study of SangShuPing coal mine. *Energy* **2023**, *266*, 126522.
(13) Wang, X. P.; Zhang, C.; Deng, J.; Su, C.; Gao, Z. Z. Analysis of Factors Influencing Miners' Unsafe Behaviors in Intelligent Mines using a Novel Hybrid MCDM Model. *Int. J. Environ. Res. Public Health* **2022**, *19*, 7368.
(14) Zhou, S. Y.; Gao, J. C.; Luo, Z. M.; Hu, S. T.; Wang, L.; Wang, T. Role of ferromagnetic metal velvet and DC magnetic field on the explosion of a C_3H_8/air mixture-effect on reaction mechanism. *Energy* **2022**, *239*, 122218.
(15) Cao, W. G.; Li, W. J.; Yu, S.; Zhang, Y.; Shu, C. M.; Liu, Y. F.; Luo, J. W.; Bu, L. T.; Tan, Y. X. Explosion venting hazards of temperature effects and pressure characteristics for premixed hydrogen-air mixtures in a spherical container. *Fuel* **2021**, *290*, 120034.
(16) Lu, K. L.; Chen, X. K.; Luo, Z. M.; Wang, Y. Y.; Su, Y.; Zhao, T. L.; Xiao, Y. The inhibiting effects of sodium carbonate on coal dust deflagration based on thermal methods. *Fuel* **2022**, *315*, 123122.
(17) Akram, M.; Kishore, K. V.; Kumar, S. Laminar burning velocity of propane/CO_2/N_2-air mixtures at elevated temperatures. *Energy Fuels* **2012**, *26*, 5509−5518.
(18) Cao, W. G.; Li, W. J.; Zhang, Y.; Zhou, Z. H.; Zhao, Y. M.; Yang, Z. X.; Liu, X. S.; Yu, S.; Tan, Y. X. Experimental study on the explosion behaviors of premixed syngas-air mixtures in ducts. *Int. J. Hydrogen Energy* **2021**, *46*, 23053−23066.
(19) Chen, Z.; Qin, X.; Xu, B.; Ju, Y.; Liu, F. Studies of radiation absorption on flame speed and flammability limit of CO_2 diluted methane flames at elevated pressures. *Proc. Combust. Inst.* **2007**, *31*, 2693−2700.
(20) Kishore, V. R.; Muchahary, R.; Ray, A.; Ravi, M. R. Adiabatic burning velocity of H_2-O_2 mixtures diluted with CO_2/N_2/Ar. *Int. J. Hydrogen Energy* **2009**, *34*, 8378−8388.
(21) Cui, C. B.; Shao, S.; Jiang, S. G.; Zhang, X. Experimental study on gas explosion suppression by coupling CO_2 to a vacuum chamber. *Powder Technol.* **2018**, *335*, 42−53.
(22) Di Benedetto, A.; Cammarota, F.; Di Sarli, V.; Salzano, E.; Russo, G. Reconsidering the flammability diagram for CH_4/O_2/N_2 and CH_4/O_2/CO_2 mixtures in light of combustion-induced Rapid Phase Transition. *Chem. Eng. Sci.* **2012**, *84*, 142−147.
(23) Di Benedetto, A.; Di Sarli, V.; Salzano, E.; Cammarota, F.; Russo, G. Explosion behavior of CH_4/O_2/N_2/CO_2 and H_2/O_2/N_2/CO_2 mixtures. *Int. J. Hydrogen Energy* **2009**, *34*, 6970−6978.
(24) Wang, Z. R.; Ni, L.; Liu, X.; Jiang, J. C.; Wang, R. Effects of N_2/CO_2 on explosion characteristics of methane and air mixture. *J. Loss Prev. Process* **2014**, *31*, 10−15.
(25) Luo, Z. M.; Wei, C. C.; Wang, T.; Su, B.; Cheng, F. M.; Liu, C. C.; Wang, Y. C. Effects of N_2 and CO_2 dilution on the explosion behavior of liquefied petroleum gas (LPG)-air mixtures. *J. Hazard. Mater.* **2021**, *403*, 123843.
(26) Xie, Y. L.; Wang, J. H.; Xu, N.; Yu, S. B.; Huang, Z. H. Comparative study on the effect of CO_2 and H_2O dilution on laminar burning characteristics of CO/H_2/air mixtures. *Int. J. Hydrogen Energy* **2014**, *39*, 3450−3458.
(27) Liao, S.; Jiang, D. M.; Cheng, Q.; Gao, J.; Hu, Y. Approximations of flammability characteristics of liquefied petroleum gas-air mixture with exhaust gas recirculation (EGR). *Energy Fuels* **2005**, *19*, 32400.
(28) Li, M. H.; Xu, J. C.; Wang, C. J.; Wang, B. Z. Thermal and kinetics mechanism of explosion mitigation of methane-air mixture by N_2/CO_2 in a closed compartment. *Fuel* **2019**, *255*, 115747.
(29) Gant, S. E.; Pursell, M. R.; Lea, C. J.; Fletcher, J.; Rattigan, W.; Thyer, A. M.; Connolly, S. Flammability of hydrocarbon and carbon dioxide mixtures. *Process Saf. Environ.* **2011**, *89*, 472−481.
(30) Mitu, M.; Brandes, E.; Hirsch, W. Mitigation effects on the explosion safety characteristic data of ethanol/air mixtures in closed vessel. *Process Saf. Environ.* **2018**, *117*, 190−199.
(31) Luo, Z. M.; Wang, T.; Tian, Z. H.; Cheng, F. M.; Deng, J.; Zhang, Y. T. Experimental study on the suppression of gas explosion using the gas-solid suppressant of CO_2/ABC powder. *J. Loss Prev. Process* **2014**, *30*, 17−23.
(32) Liu, G. Y.; Zhou, J. H.; Wang, Z. H.; Yang, W.; Liu, J.; Cen, K. Adiabatic laminar burning velocities of C_3H_8-O_2-CO_2 and C_3H_8-O_2-N_2 mixtures at ambient conditions-PART II: Mechanistic interpretation. *Fuel* **2020**, *276*, 117946.
(33) Mitu, M.; Giurcan, V.; Razus, D.; Prodan, M.; Oancea, D. Propagation Indices of Methane-Air Explosions in Closed Vessels. *J. Loss Prev. Process* **2017**, *47*, 110−119.
(34) Luo, Z. M.; Su, B.; Li, Q.; Wang, T.; Kang, X. F.; Cheng, F. M.; Gao, S. S.; Liu, L. T. Micromechanism of the initiation of a multiple flammable gas explosion. *Energy Fuels* **2019**, *33*, 7738−7748.
(35) Shi, X. Q.; Zhang, Y. T.; Chen, X. K.; Zhang, Y. B.; Rui, R.; Guo, R. Z.; Zhao, T. L.; Deng, Y. Numerical simulation on response characteristics of coal ignition under the disturbance of fluctuating heat. *Combust. Flame* **2022**, *237*, 111870.
(36) Bird, J. O. Ideal gas laws. In *Newnes engineering science pocket book*; ButterworthHeinemann, 1987, pp 317−321.
(37) Pekalski, A. A.; Schildberg, H. P.; Smallegange, P. S. D.; Lemkowitz, S. M.; Zevenbergen, J. F.; Braithwaite, M.; Pasman, H. J. Determination of the explosion behaviour of methane and propene in air or oxygen at standard and elevated conditions. *Process Saf. Environ.* **2005**, *83*, 421−429.
(38) Lu, K. L.; Chen, X. K.; Luo, Z. M.; Wang, Y. Y.; Su, Y.; Zhao, T. L.; Xiao, Y. Inhibiting effects investigation of pulverized coal explosion using melamine cyanurate. *Powder Technol.* **2022**, *401*, 117300.
(39) Sanogo, O.; Delfau, J. L.; Akrich, R.; Vovelle, C. Experimental and modeling study of the effect of CF_3CHFCF_3 on the chemical structure of a methane-oxygen-argon flame. *Combust. Sci. Technol.* **1997**, *122*, 33−62.
(40) Shi, Z. W.; Zheng, L. G.; Zhang, J. L.; Miao, Y. X.; Wang, X.; Wang, Y.; Tang, S. Effect of initial pressure on methane/air deflagrations in the presence of $NaHCO_3$ particles. *Fuel* **2022**, *325*, 124910.
(41) Wang, J. H.; Huang, Z. H.; Kobayashi, K.; Ogami, O. Laminar burning velocities and flame characteristics of CO-H_2-CO_2-O_2 mixtures. *Int. J. Hydrogen Energy* **2012**, *37*, 19158−19167.
(42) Razus, D.; Brinzea, V.; Mitu, M.; Oancea, D. Burning Velocity of Liquefied Petroleum Gas (LPG)-Air Mixtures in the Presence of Exhaust Gas. *Energy Fuels* **2010**, *24*, 1487−1494.

https://doi.org/10.1021/acsomega.2c07053
ACS Omega 2023, 8, 10863−10874

(43) Zhenmin, L.; Wang, T.; Gao, Z. J.; Su, B. Influence of multi-component combustible gases on explosion characteristics and free radical emission spectrum of CH_4. *China Saf. Sci. J.* **2020**, *30*, 1−7.
(44) Su, B.; Luo, Z. M.; Wang, T.; Yan, K.; Cheng, F. M.; Deng, J. Coupling analysis of the flame emission spectra anrd explosion characteristics of CH_4/C_2H_6/air mixtures. *Energy Fuels* **2020**, *34*, 920−928.
(45) Wang, L. D.; Li, P.; Zhang, C. H.; Tang, H. C.; Ye, B.; Li, X. Y. Transient Emission Spectra from OH, CH and C_2 Free Radicals in the Combustion Reaction of n-Decane. *Spectrosc. Spect. Anal.* **2012**, *32*, 1166−1169.
(46) Peyman, Z.; Kianoosh, Y. Effects of pressure and carbon dioxide, hydrogen and nitrogen concentration on laminar burning velocities and NO formation of methane-air mixtures. *J. Mech. Sci. Technol.* **2014**, *28*, 377−386.
(47) Higgins, B.; McQuay, M. Q.; Lacas, F.; Candel, S. An experimental study on the effect of pressure and strain rate on CH chemiluminescence of premixed fuel-lean methane/air flames. *Fuel* **2001**, *11*, 1583.
(48) Keda, Y.; Kojima, J.; Nakajima, T. Local chemilumines cence spectra measurement in laminar methane/air and propane/air premixed flames. *Trans. Jpn. Soc. Mech. Eng.* **2003**, *69*, 200−213.
(49) Su, B.; Luo, Z. M.; Wang, T.; Zhang, J.; Cheng, F. M. Experimental and principal component analysis studies on minimum oxygen concentration of methane explosion. *Int. J. Hydrogen Energy* **2020**, *45*, 12225−12235.
(50) Doll, J.; George, T.; Miller, W. Complex-valued classical trajectories for reactive tunneling in three-dimensional collisions of H and H_2. *J. Chem. Phys.* **1973**, *58*, 1343−1351.
(51) Halter, F.; Foucher, F.; Landry, L.; Mounaïm-Rousselle, C. Effect of dilution by nitrogen and/or carbon dioxide on methane and iso-octane air flames. *Combust. Sci. Technol.* **2009**, *181*, 813−827.
(52) Rathnam, R. K.; Elliott, L. K.; Wall, T. F.; Liu, Y.; Moghtaderi, B. Differences in reactivity of pulverised coal in air (O_2/N_2) and oxy-fuel (O_2/CO_2) conditions. *Fuel Process. Technol.* **2009**, *90*, 797−802.
(53) Ranganathan, S.; Lee, M.; Akkerman, V.; Rangwala, A. S. Suppression of premixed flames with inert particles. *J. Loss Prev. Process* **2015**, *35*, 46−51.
(54) Zhang, B.; Xiu, G.; Bai, C. Explosion characteristics of argon/nitrogen diluted natural gas-air mixtures. *Fuel* **2014**, *124*, 125−132.

https://doi.org/10.1021/acsomega.2c07053
ACS Omega 2023, 8, 10863−10874